

Two new ultracool benchmark systems from *WISE*+2MASS

J. I. Gomes,¹* D. J. Pinfield,¹ F. Marocco,¹ A. C. Day-Jones,^{1,2} B. Burningham,¹
Z. H. Zhang,¹ H. R. A. Jones,¹ L. van Spaandonk¹ and D. Weights¹

¹Centre for Astrophysics Research, University of Hertfordshire, College Lane, Hatfield, Hertfordshire AL10 9AB, UK

²Departamento de Astronomía, Universidad de Chile, Camino del Observatorio 1515, Santiago, Chile

Accepted 2013 February 25. Received 2013 February 25; in original form 2012 August 30

ABSTRACT

We have used the Two-Micron All-Sky Survey and the *Wide-field Infrared Survey Explorer* to look for ultracool dwarfs that are part of multiple systems containing main-sequence stars. We cross-matched L dwarf candidates from the surveys with Hipparcos and Gliese stars, finding two new systems. The first system, G255-34AB, is an L2 dwarf companion to a K8 star, at a distance of 36 pc. We estimate its bolometric luminosity as $\log L/L_{\odot} = -3.78 \pm 0.045$ and $T_{\text{eff}} = 2080 \pm 260$ K. The second system, GJ499ABC, is a triple, with an L5 dwarf as a companion to a binary with an M4 and K5 star. These two new systems bring the number of L dwarf plus main-sequence star multiple systems to 24, which we discuss. We consider the binary fraction for L dwarfs and main-sequence stars, and further assess possible unresolved multiplicity within the full companion sample. This analysis shows that some of the L dwarfs in this sample might actually be unresolved binaries themselves, since their M_J appears to be brighter than the expected for their spectral types.

Key words: surveys – brown dwarfs – stars: low-mass.

1 INTRODUCTION

In the last few years, an increasing number of binary systems with ultracool components have been discovered and studied. Ultracool dwarfs (UCDs) are defined as dwarf stars with spectral types of M7 or later, and include substellar brown dwarfs (Baraffe et al. 1998; Jones & Steele 2001; masses $< 0.072 M_{\odot}$) and some very low mass stars. UCDs populate the lower temperature range, from effective temperatures $T_{\text{eff}} \sim 2400$ –500 K (Kirkpatrick 2005).

Beyond the late M dwarfs, lies the L dwarf sequence, which have T_{eff} ranging from 2250 to 1400 K (Kirkpatrick et al. 1999). While for earlier types there can be some hydrogen burning very low mass stars, most L dwarfs will be substellar-mass brown dwarfs. The sequence extends into the cooler T dwarf regime and to T_{eff} of ~ 500 K (Lucas et al. 2010). The Y dwarf spectral type, first proposed by Kirkpatrick et al. (1999) has only recently seen its first confirmed objects with Cushing et al. (2011) discovering six Y dwarfs from the *Wide-field Infrared Survey Explorer* (*WISE*). More recently Kirkpatrick et al. (2012) presented seven more Y dwarfs from *WISE*, bringing the current total of confirmed objects to 13. The *WISE* (Wright et al. 2010) satellite has surveyed the entire sky in four infrared (IR) bands (*W1*, *W2*, *W3* and *W4*), at wavelengths of 3.4, 4.6, 12 and 22 μm . Bands *W1* and *W2* give the best sensitivity to the coolest brown dwarfs due to the strong absorption centred at 3.3 μm (*W1*) owing to methane for objects with $T_{\text{eff}} < 1500$ K.

At 4.6 μm (*W2*), however, there is no methane; as such the *W1* – *W2* colour is very sensitive to cool brown dwarfs.

Several other large-scale optical and near-IR (NIR) surveys have already proved to be effective tools at finding and studying large populations of UCDs: the Two-Micron All-Sky Survey (2MASS; Skrutskie et al. 2006) and the Deep Near Infrared Survey of the Southern Sky (DENIS; Epchtein et al. 1997) in the NIR, and the Sloan Digital Sky Survey (SDSS; York et al. 2000) in the optical. As brown dwarfs cool and fade significantly over time this leads to a mass–age degeneracy, with lower mass younger brown dwarfs having similar T_{eff} and luminosity to higher mass, older ones. Measuring atmospheric properties (T_{eff} , $\log g$, [m/H]) of brown dwarfs in order to infer mass and age is thus crucial. Using NIR and optical spectra and model fitting techniques, one can attempt to constrain physical properties for UCDs. However, dust condensation, non-equilibrium chemistry and complex molecular opacities make it very challenging to accurately model such atmospheres, and the reliable fitting of properties with spectral models is not currently reliable (Pinfield et al. 2012).

One way to overcome these problems is to identify UCDs whose properties can be estimated in a relatively independent way. We refer to such objects as benchmark UCDs. They can be used as a testbed for prevailing theories and models. UCDs that are wide companions to main sequence (MS) stars of the Galactic disc are fairly numerous, cover the full range of age and metallicity, and are therefore particularly useful benchmarks. van Biesbroeck (1961) was one of the first to search for these systems and the method used has been followed by many other successful studies (e.g. Gizis,

*E-mail: j.gomes@herts.ac.uk

Kirkpatrick & Wilson 2001; Kirkpatrick et al. 2001; Wilson et al. 2001; Pinfield et al. 2006, 2012; Burningham et al. 2009; Faherty et al. 2009, 2010; Day-Jones et al. 2011).

Since the peak of the spectral energy distribution (SED) of L dwarfs occurs at NIR wavelengths, 2MASS and *WISE* are ideal to discover large numbers of these objects. In fact, both surveys cover the whole sky and are well matched which makes them a powerful tool to detect L dwarfs. Despite their relatively large pixel sizes of 1 arcsec in 2MASS and 1.375 arcsec in *WISE*, the 10 year baseline between these surveys also makes it possible to accurately determine proper motions. This is important as it allows confirmation of the binarity in these systems.

We present here the measurement of proper motion for 10 L dwarf candidates and the discovery of two new wide binary systems. Section 2 describes the technique used to identify these systems and how we assessed their common proper motion, describing our follow-up spectroscopic observations whilst in Section 3 we present the two new binary systems in more detail, addressing the issue of possible contamination. In Section 4, we discuss results, estimate a binary fraction for these type of objects and investigate the possibility that some known UCDs with MS stars companions are actually unresolved objects. Finally, our conclusions are presented in Section 5.

2 CANDIDATES SELECTION

2.1 L dwarfs selection

The UCD candidates were selected using NIR photometry available from the 2MASS all-sky point catalogue. This data base is ideal to search for L dwarfs as it covers the whole sky and the NIR *JHKs* filters sample the peak of the SED of such objects. Colour-selection criteria were applied to obtain a first sample of L dwarf candidates. This selection required the following:

$$0.5 \leq J - H \leq 1.6$$

$$1.1 \leq J - K \leq 2.8$$

$$0.4 \leq H - K \leq 1.1$$

$$J - H \leq 1.75(H - K) + 0.37$$

$$J - H \geq 1.65(H - K) - 0.35.$$

We only consider candidates with a *J*-band magnitude ≤ 16.0 . These constraints were chosen based on the colours of known L dwarfs from Dwarf Archives.¹ To avoid source confusion and contamination from MS and giant stars some high-density regions were excluded, such as the galactic plane ($b \geq |25^\circ|$) and the Large and Small Magellanic Clouds. Two other reddened and overcrowded regions were also removed. Information about these regions can be seen in Table 1. The equatorial poles were also avoided ($\delta \geq |86^\circ|$) as 2MASS is not complete in these regions for optical cross-matching. The total area of the sky included in the first sample was 22, 178 deg² or 53 per cent of the sky.

We have kept objects with no optical counterpart within 5 arcsec in the USNO-A2.0 catalogue or, if they do have counterparts, with $R - K > 5.5$. By doing this, we ensure that all detections with optical counterparts are of spectral types later than M6 as these objects have extremely red colours in both the optical and IR domain due to their low T_{eff} . A signal-to-noise ratio (S/N) criterion

Table 1. Uncatalogued regions that have been removed from the initial sample.

l_{min}	l_{max}	b_{min}	b_{max}
0	96	-16	16
150	180	10	13
180	360	-13	13
199	214	-13	-27
308	310	13	16

was imposed to exclude low-quality photometric data ($S/N > 5$ for all the bands). Flags including $\text{ccflg}=000$, $\text{prox}>6$, $\text{gal.contam}=0$ and $\text{mpflg}=0$ were applied to make sure that the sources were unaffected by known artefacts, such as diffraction spikes from nearby bright stars, and to exclude extended sources and known minor planets. This first sample of possible UCD candidates encompasses 28 023 objects.

We find that 269 of the 602 known L dwarfs were present in our initial list. The remaining ones did not make it through our initial cuts, either because they had *J*-band magnitudes larger than 16, Galactic latitudes outside our limit or they did not pass the quality flags imposed. It is important to note that only 36 were excluded based on their colours; thus, the vast majority of L dwarfs have NIR colours inside the colour space we initially defined, thus validating our method.

2.2 Selection of binaries

2.2.1 Assessing photometry and separation

In order to search for companions to our L dwarf candidates, we selected a sample of MS stars from different catalogues, namely the Hipparcos (van Leeuwen 2007) and Gliese (Gliese & Jahreiss 1991) catalogues. We selected only Hipparcos stars within 50 pc as we only want to consider pairs up to this distance, whilst Gliese stars have a maximum distance of 25 pc (due to limitations of the catalogue itself). The sample consists only of F, G and K stars. Assuming the star's distance, we looked for L dwarf companions up to an on-sky separation corresponding to 20 000 au and angular separations of up to 10 arcmin, finding 572 possible pairs.

Next, we plot the UCD candidates on a colour-magnitude diagram (CMD), in order to assess if their photometry was consistent with a real UCD at the companion's distance. Using the distance of the primary star, we calculated M_J and with the $J - K$ colour, obtained the plot shown in Fig. 1. Following the method used by Pinfield et al. (2006), we selected pairs where the L dwarf candidate was within a specific region. This region was defined using a sample of L dwarfs with known parallax, or with distances inferred from companion stars (Kirkpatrick et al. 2001; Wilson et al. 2001) and the M_J range from Knapp et al. (2004). We considered all of our pairs and using the CMD, identified 25 possible MS star-UCD binary systems.

2.2.2 Cross-checking in other surveys

In order to account for previous analysis, look for multi-epoch imaging data and additional colour constraints for the UCD candidates, we performed a cross-check with multiple NIR and optical surveys, specifically the SuperCOSMOS Science Archive, SDSS, Digitized Sky Survey, DENIS, *WISE*, the UKIRT Infrared Deep Sky Survey (UKIDSS, Lawrence et al. 2007) and the SIMBAD data base. We

¹ See <http://DwarfArchives.org>.

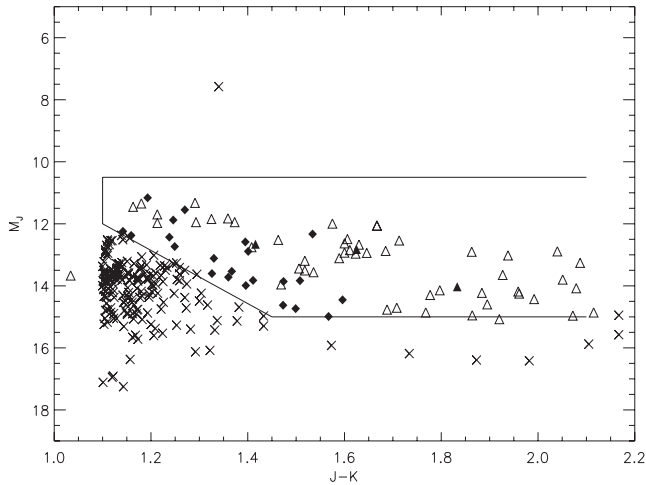


Figure 1. M_J versus $J - K$ CMDs. The UCDs from the candidate pairs are shown as crosses. Inside the selection box, the filled triangles are the three known L dwarfs that turn up in our sample as possible binaries, the filled diamonds are UCDs candidates not confirmed and not in the dwarfarchive.org. The open triangles represent other UCDs with known parallax measurements from Dwarf Archives and are displayed for comparison purposes only.

excluded nine of the selected UCD candidates, as they were classified as galaxies or flare stars. Of the remaining 16 candidates, three were found to be known L dwarfs, another three have measured proper motions in the literature and the remaining 10 do not have any proper motion measurements. This cross-check also allowed us to select the best epochs to calculate proper motions for the latter 10 UCD candidates. We used 2MASS as the first epoch and WISE as the second epoch when possible. Being the most recent NIR survey, WISE allows us to have a larger baseline between the two epochs and thus more accurate proper motion measurements. If WISE images were not the most suitable ones, we then selected the second epoch from the other surveys. All images were chosen taking into account the largest baselines possible and a reasonable number of

appropriately positioned bright stars that could be used as reference objects.

2.2.3 Assessing common proper motion

Proper motion calculations were made using standard IRAF routines. Measuring the positions of an average of 12 reference stars, we have used the IRAF routine GEOMAP to derive the spatial transformation between the two epochs. Then, the routine GEOXYTRAN applied these transformations to the coordinates of the UCD candidate, and estimated how they changed between epochs. The uncertainties for this process are the combination of the rms scatter associated with the coordinates transformation and the centroiding accuracies. Amongst our UCD candidates some had proper motions available in the literature. We compared our results with the published ones to check for consistency and then use the value with the smaller uncertainty.

To verify if a pair has a common proper motion, we compared the proper motion in right ascension and declination of each component, taking into account the uncertainties associated with each measurement. We consider that two objects have common proper motion if they match to within $\sigma < 2$, σ being the difference between their individual proper motions across the sky divided by the errors. In Table 2, we present the proper motions for all the candidates. Out of this sample, only two were found to have common proper motion with their primary star. The UCDs in these pairs are 2MASS J133245.30+745944.1 and 2MASS J130541.07+204639.4 (hereafter 2MASS J1332+7459 and 2MASS J1305+2046, respectively). Information about these is shown in Tables 3 and 4. In one of the cases, the UCD is an uncatalogued L dwarf, whilst the other is classified as an $L4 \pm 2$ by Cruz et al. (2003). Our sample also included one known binary discovered by Faherty et al. (2010), G62-33.

2.3 Follow-up observations

The 2MASS J1332+7459 UCD candidate was observed with the 3.58-m Telescopio Nazionale Galileo (TNG) in combination with

Table 2. Proper motion measurements for the L dwarf candidates.

Name of L dwarf candidates	RA (J2000)	Dec. (J2000)	pm _{RA}	pm _{Dec.}	Possible primary	Notes
2MASS J003142.93-630818.6	00 31 42.94	-63 08 18.6	133 ± 8	-88 ± 8	HIP 2540	a
2MASS J071051.38-492212.2	07 10 51.38	-49 22 12.4	-14 ± 12	121 ± 9	HIP 34739	a
2MASS J074231.27+180816.8	07 42 31.27	+18 08 16.8	57 ± 31	-78 ± 15	HIP 37622	a
2MASS J100428.24-114648.9	10 04 28.25	-11 46 49.1	-130 ± 15	91 ± 15	HIP 49366	a
2MASS J132434.95+545615.2	13 24 34.94	+54 56 15.4	2 ± 12	7 ± 10	HR 5055	a
2MASS J134154.14-014553.1	13 41 54.15	-01 45 53.2	-18 ± 5	-34 ± 6	HIP 66886	a
2MASS J134751.79-104433.7	13 47 51.79	-10 44 33.7	-432 ± 28	-9 ± 18	HIP 67344	a
2MASS J190536.28-370546.3	19 05 36.29	-37 05 46.3	-0.2 ± 2	-7 ± 6	HR 7227	a
2MASS J073523.28+315050.6	07 35 23.18	+31 50 50.6	14 ± 10	30 ± 8	HD 60179C	a
2MASS J133245.30+745944.1	13 32 45.31	+74 59 44.2	-471 ± 28	39 ± 22	G255-34	b
2MASS J130541.07+204639.4	13 05 41.07	+20 46 39.4	-23 ± 17	73 ± 27	GJ499AB	b
2MASS J083204.51-012836.0	08 32 04.51	-01 28 36.1	64 ± 13	27 ± 15	GJ3504	c
2MASS J132044.27+040904.5	13 20 44.28	+04 09 04.7	-483 ± 19	211 ± 17	HIP 65121	d
2MASS J112149.24-131308.4	11 21 49.25	-13 13 08.4	-509 ± 10	-81 ± 10	GJ3655	e
2MASS J022128.59-683140.0	02 21 28.61	-68 31 40.1	46 ± 6	-6 ± 17	HIP 11001	f
2MASS 063447.73-582955.3	06 34 47.73	-58 29 55.3	73 ± 9	-21 ± 9	HIP 31300	g

Notes. (a) New L dwarf candidates with new proper motion measurements; (b) new common proper motion pairs, here presented; (c) proper motion from Casewell, Jameson & Burleigh (2008); (d) proper motion from Jameson et al. (2008) and common proper motion pair discovered by Faherty et al. (2010); (e) proper motion from Salim & Gould (2003); (f) proper motion from Faherty et al. (2009); (g) proper motion from Roeser, Demleitner & Schilbach (2010).

Table 3. Properties of the system G255-34AB.

Parameter	Value
Name	2MASS J1332+7459 (G255-34B)
RA (J2000)	13 32 45.31
Dec. (J2000)	+74 59 44.2
<i>J</i>	15.103 ± 0.041
<i>H</i>	14.116 ± 0.034
<i>K</i>	13.569 ± 0.032
<i>W1</i>	13.170 ± 0.025
<i>W2</i>	12.916 ± 0.032
<i>W1</i> – <i>W2</i>	0.254
<i>J</i> – <i>W2</i>	2.187
<i>H</i> – <i>W2</i>	1.200
μ_{RA}	−471.296 ± 28.489 mas yr ^{−1}
$\mu_{\text{Dec.}}$	38.773 ± 22.113 mas yr ^{−1}
SpType	L2
log <i>L</i> / <i>L</i> _⊙	−3.780 ± 0.045
<i>T</i> _{eff}	2080 ± 260 K
Name	G255-34A (HIP 66074)
RA (J2000)	13 32 41.02
Dec. (J2000)	+75 00 24.81
<i>B</i>	11.53
<i>V</i>	10.23
<i>R</i>	9.7
<i>I</i>	9.2
<i>J</i>	7.910 ± 0.024
<i>H</i>	7.302 ± 0.033
<i>K</i>	7.182 ± 0.016
μ_{RA}	−438.50 ± 1.33 mas yr ^{−1}
$\mu_{\text{Dec.}}$	49.82 ± 1.05 mas yr ^{−1}
Parallax	27.62 ± 1.14 mas
Distance	36.21 ± 1.50 pc
SpType	K8
<i>U</i>	−49.7 km s ^{−1}
<i>V</i>	−63.8 km s ^{−1}
<i>W</i>	−17.6 km s ^{−1}
<i>V</i> total	82.7 km s ^{−1}
<i>T</i> _{eff}	4368 K

the Device Optimized for the LOW RESolution (DOLORES or LRS for short) on 2011 May 13. LRS was equipped with a 2048 × 2048 E2V 4240 CCD and the LR-R grating with a resolving power of $R \sim 700$, centred at 7400 Å. A slit width of 1.0 arcsec was used with a seeing of ~ 1.1 arcsec during the observations. This setup provided a wavelength coverage from 5200 to 10 400 Å, with a dispersion of 2.7 Å per pixel and a resolution of 3.8 Å at the central wavelength.

The spectra were reduced in the following way: the average bias and flat-field correction was carried out using the FIGARO package from STARLINK using average bias and halogen frames, taken on the same night. The spectral reduction suite PAMELA was used for the optimal extraction of the spectra.

A neon and mercury arc lamp exposure at the same position as the targets allowed us to establish an accurate wavelength scale for each of the five spectra obtained. We used MOLLY, a 1D astronomical spectral analysis package, to fit the arc frame with a fourth-order polynomial, giving an rms of 0.17 Å. The spectral resolution was measured by the full width at half-maximum of the arc lines, using an average of 10 lines located across the entire wavelength range. The individual spectra were flux calibrated using the nearby spectrophotometric standard flux star GRW +70d5824. The final spectrum is a variance weighted average of the five individual spectra.

Table 4. Properties of the system GJ499ABC.

Parameter	Value
Name	J1305+2046 (GJ499C)
RA (J2000)	13 05 41.07
Dec. (J2000)	+20 46 39.4
<i>J</i>	15.20 ± 0.053
<i>H</i>	14.04 ± 0.042
<i>K</i>	13.37 ± 0.039
<i>W1</i>	12.540 ± 0.026
<i>W2</i>	12.153 ± 0.025
<i>W1</i> – <i>W2</i>	0.387
<i>J</i> – <i>W2</i>	3.047
<i>H</i> – <i>W2</i>	1.887
μ_{RA}	−42.61 ± 32.1 mas yr ^{−1}
$\mu_{\text{Dec.}}$	103.25 ± 15.4 mas yr ^{−1}
SpType	L5
log <i>L</i> / <i>L</i> _⊙	−4.23
<i>T</i> _{eff}	1574 ± 170 K
Name	GJ499AB (HIP 63942)
RA (J2000)	13 06 15.43
Dec. (J2000)	+20 43 44.40
<i>V</i> ₁	9.40
<i>J</i> ₁	6.89 ± 0.01
<i>H</i> ₁	6.27 ± 0.01
<i>K</i> ₁	6.05 ± 0.01
<i>V</i> ₂	14.90
<i>J</i> ₂	10.25 ± 0.10
<i>H</i> ₂	9.75 ± 0.10
<i>K</i> ₂	9.55 ± 0.10
μ_{RA}	−49.17 ± 1.7 mas yr ^{−1}
$\mu_{\text{Dec.}}$	101.14 ± 1.1 mas yr ^{−1}
Parallax	53.18 ± 1.73 mas
Distance	18.80 ± 0.61 pc
SpTypeA	K5
Sp TypeB	M4
<i>T</i> _{eff}	4210 K
<i>U</i>	−9.0 km s ^{−1}
<i>V</i>	5.1 km s ^{−1}
<i>W</i>	−1.4 km s ^{−1}
<i>V</i> total	10.4 km s ^{−1}

Notes. *V*₁, *J*₁, *H*₁ and *K*₁ refer to GJ499A whereas *V*₂, *J*₂, *H*₂ and *K*₂ refer to GJ499B.

3 BINARY CANDIDATES

3.1 G255-34AB

3.1.1 Properties of the *L* dwarf G255-34B

To measure the UCDs spectral type, we have compared the optical spectra obtained at the TNG to standard template spectra from the *L* dwarf sequence defined in Kirkpatrick et al. (1999). The comparison was done using four different subclasses, L0, L1, L2 and L3, using the following objects as standards: for L0, 2MASP J034532+254023; for L1, 2MASSW J1439284+192915; for L2, Kelu1 (all three from Kirkpatrick et al. 1999) and for L3, DENIS-P J1058.7–1548 (Delfosse et al. 1997). In order to define the best subclass for this dwarf, we used a χ^2 minimization and the goodness-to-fit statistic, G_k , defined in Cushing et al. (2008). Whereas the χ^2 minimization classifies this UCD as an L2 dwarf, the method described in Cushing et al. (2008) classifies it as an L1. The fit of the observed spectrum to the template spectra can be seen in Fig. 2. The fitting was done for the wavelength range 6300–9500 μm.

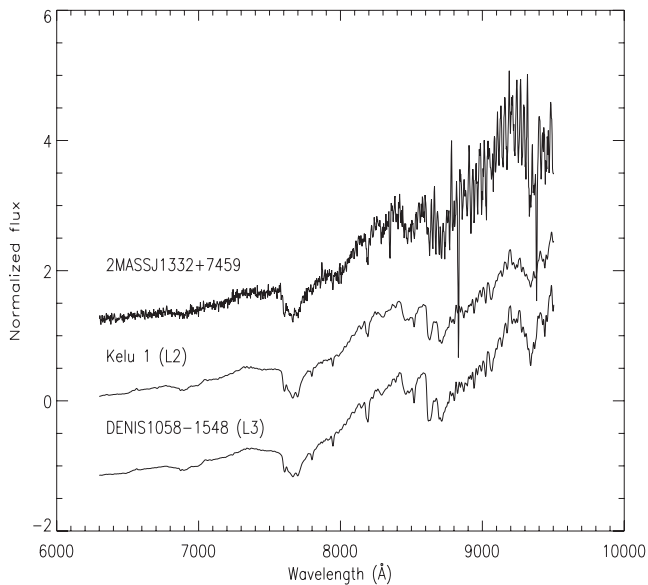


Figure 2. Optical spectrum of the 2MASS J1332+7459 dwarf, with the standard spectra of an L2 dwarf, Kelu 1, and an L3 dwarf, DENIS 1058–1548. The spectra has been displaced vertically in order to better compare them. The fit has been made for the wavelength range 6300–9500 Å.

Secondly, we estimated three spectral ratios, CrH-a, Rb-b/TiO-b and Cs-a/VO-b, defined in Kirkpatrick et al. (1999) for L dwarfs with spectral types < L5. The values for these ratios are 1.29, 1.08 and 0.91, respectively, usually associated with L2 dwarfs.

Looking more closely at the spectrum of G255-34B, we see that despite showing TiO λ 8432, CrH λ 8611 and FeH λ 8692 lines all similar in strength, typical of L1 dwarfs, the spectrum actually shows most of the spectral key features of the subclass L2 (Kirkpatrick et al. 1999). As an example, we refer to the distinctly sloped part of the spectrum between 7800 and 8000 Å and the TiO lines λ 8432 and λ 7053 that become weaker and disappear, respectively.

Finally, we checked the two *WISE* bands to derive a spectral type in an independent way, using colour–spectral type plots. According to the $W1 - W2$ versus spectral type plot of Kirkpatrick et al. (2011), the L dwarf, showing a $W1 - W2$ colour of 0.254, should have a spectral type between M5 and L4. However, looking at the colours, $J - W2$ and $H - W2$, versus spectral type plots, it can be seen that the UCD colours are similar to the ones shown by L0–L3 dwarfs. These conclusions are consistent with the value obtained using our previous method. Taking all these spectral classification diagnostics into account, we here classify this UCD as an L2 dwarf.

To determine the bolometric luminosity, we have combined the optical spectra of the L dwarf with the photometry available. In the NIR part of the spectrum, we used *JHK* photometry from 2MASS, extending to the mid-IR with *WISE* bandpasses *W1* and *W2*. We followed the method described in Marocco et al. (2010) to estimate the bolometric luminosity. First, we created synthetic spectra for those regions of the electromagnetic spectrum lacking observations (NIR and mid-IR). We used the models of Hubeny & Burrows (2007) since these cover a temperature range between 700 and 1900 K, and have considered that the models are still valid for the typically larger temperature values of early L dwarfs (up to 2250 K). We allowed for different values of $\log g$, 4.5, 5.0 and 5.5, and assumed $K_{zz} = 10^2, 10^4$ and $10^6 \text{ cm}^{-2} \text{ s}^{-1}$ (eddy diffusion coefficient). Secondly, we estimated the difference in flux between

our models and the flux given by the available photometry, known as the scaling factor. Comparing this value with the scaling factor given by the distance assumed for the L dwarf and the radius range adopted (between $0.8 R_{\text{Jup}}$ and $1.2 R_{\text{Jup}}$), we only considered models for which the average scaling factor was within a certain interval. Thirdly, combining the synthetic spectra with the observed one, we calculated the bolometric flux, luminosity and temperature range from the radius range. We then excluded the models in which the temperature was at least 100 K outside the constrained range. The final step takes into account only the remaining models and using the mean flux, we have estimated a final bolometric luminosity of $6.38 \pm 0.67 \times 10^{29} \text{ erg s}^{-1}$ or $1.67 \pm 0.17 \times 10^{-4} L_{\odot}$. Taking a radius range of $0.8\text{--}1.2 R_{\text{Jup}}$ and the luminosity, we can derive the corresponding temperature for this L2 dwarf as $T_{\text{eff}} = 2080 \pm 260 \text{ K}$.

We have also derived the bolometric luminosity and T_{eff} for the L dwarf following this procedure: taking into account the spectral type information derived before, we estimated the *K*-band bolometric corrections using the polynomial fit of Golimowski et al. (2004) and hence the apparent bolometric magnitude of the object. Combining this with the distance, inferred from parallax measurements, we obtain the absolute bolometric magnitude and consequently, the bolometric luminosity. From the luminosity, T_{eff} can be directly calculated. The results are, for bolometric luminosity and T_{eff} , respectively, $7.14 \times 10^{29} \text{ erg s}^{-1}$ or $1.87 \times 10^{-4} L_{\odot}$, and $T_{\text{eff}} = 2106^{+250}_{-180} \text{ K}$, and are in agreement with the previous values. For the T_{eff} , we again considered a radius range of $0.8\text{--}1.2 R_{\text{Jup}}$.

3.1.2 System properties

The components of the first system are the L2 dwarf discussed in Section 3.1.1 and a K8 dwarf (Vyssotsky 1956), G255-34A, and a finder chart of these can be seen in Fig. 3. The spectral type we derived earlier for the L dwarf suggests an M_J of 12.36 ± 0.11 based on Dupuy & Liu (2012). This places it at a distance of $35.36^{+1.84}_{-1.75} \text{ pc}$, consistent with the measured parallax of the K8 primary, at $36.21 \pm 1.50 \text{ pc}$ (van Leeuwen 2007). G255-34A, a K8 dwarf, has a separation of 38.3 arcsec to the secondary, or 1364 au. Initially believed to be part of a common proper motion pair with another star by Luyten (1979), it is not considered as such by Giclas, Burnham & Thomas (1971), as can be noted in Weis (1991).

Schlafman & Laughlin (2010) have developed a way to calibrate M dwarf metallicity using photometry. Applying their method and using *V* and *Ks* magnitudes, we find [Fe/H] to be -0.29 dex . However, metallicity uncertainties are significant for photometric constraints, $\sim 0.2 \text{ dex}$. This is marginal evidence for G255-34A being slightly metal poor. Kinematics place this star outside the region defined as the Eggen box (Eggen & Iben 1989) (and representative of the young disc population) and therefore suggest old disc membership and a likely age greater than 1.5 Gyr. According to Leggett (1992), this is broadly consistent with an $[m/H] \sim -0.5$, and we employ the relationship for West’s earliest spectral type range as reasonably representative for a K8 dwarf to place a lower limit on the age of this system at $0.8 \pm 0.6 \text{ Gyr}$.

3.2 GJ499ABC

3.2.1 Properties of the L dwarf GJ499C

GJ499C is an L dwarf first discovered by Cruz et al. (2003). The proper motion for this dwarf has been estimated by some authors and the available values for this are shown in Table 5. Our own

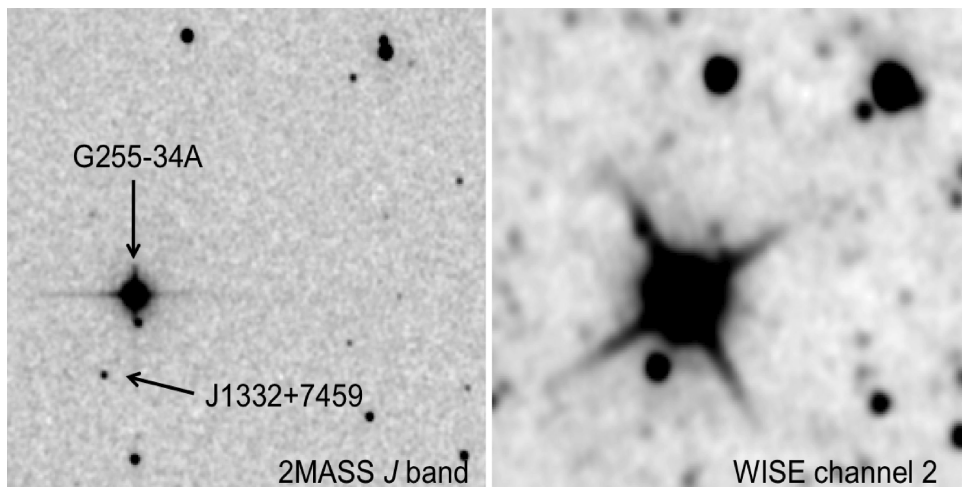


Figure 3. A 4.5 arcmin \times 4.5 arcmin finder chart for the system G255-34AB. On the left-hand panel is the *J*-band image and on the right-hand panel is the *W2* band. North is up and east is left.

Table 5. Proper motions for GJ 499C.

Ref.	μ_{RA} (mas yr $^{-1}$)	$\mu_{Dec.}$ (mas yr $^{-1}$)
Zacharias et al. 2005	-23.9 ± 9.0	-73.1 ± 9.0
Jameson et al. 2008	-23.3 ± 17.5	73.4 ± 26.9
Faherty et al. 2009	-23.0 ± 17.0	73.0 ± 27.0
Schmidt et al. 2010	-59.1 ± 33.1	73.8 ± 22.6
This paper	-42.6 ± 32.1	103.3 ± 15.4

measurements are also presented and, within the error bars, are in good agreement with the values of Jameson et al. (2008), Faherty et al. (2009) and Schmidt et al. (2010).

We have independently estimated the spectral type of the dwarf with the available spectrum from SDSS. We started by calculating the CrH-a, Rb-b/TiO-b and Cs-a/VO-b spectral ratios, with the additional colour-*d* ratio (since these are best suited to objects with spectral types $>L5$). The analysis of spectral ratios are all consistent with a spectral type of L5. We then compared the SDSS spectra with standard spectra templates, following the χ^2 minimization and the G_k factor method. We did this in order to assess if the fit to the

spectral templates was consistent with the spectral type indicated by the spectral ratios alone. We find that χ^2 minimization classifies the L dwarf as an L5, whereas the G_k factor suggests an L4 type. A final spectral type of L5 is adopted, which is in agreement with the previous result by Cruz et al. (2003), that classifies it as an $L4 \pm 2$. A finder chart for this L dwarf can be seen in Fig. 4.

Following the method described in Section 3.1.1, we have estimated the luminosity and T_{eff} for GJ499C, using bolometric corrections and a radius range of 0.8–1.2 R_{Jup} . The results are, for the luminosity and T_{eff} , 2.23×10^{29} erg s $^{-1}$ or $5.83 \times 10^{-5} L_{\odot}$, and 1574^{+190}_{-140} K, in agreement with what it is expected for L5 dwarfs.

3.2.2 System properties

The primary components of the system G499AB contain a K5 with a closely separated M4 dwarf (Reid et al. 2004), at a separation of 0.9 arcsec. According to Dupuy & Liu (2012), the mean M_J value for a L5 dwarf is 13.56 ± 0.03 , and with this we estimate a distance of $21.28^{+0.30}_{-0.28}$ pc to the GJ499 triple system. The parallax measurements from the Hipparcos catalogue (van Leeuwen 2007)

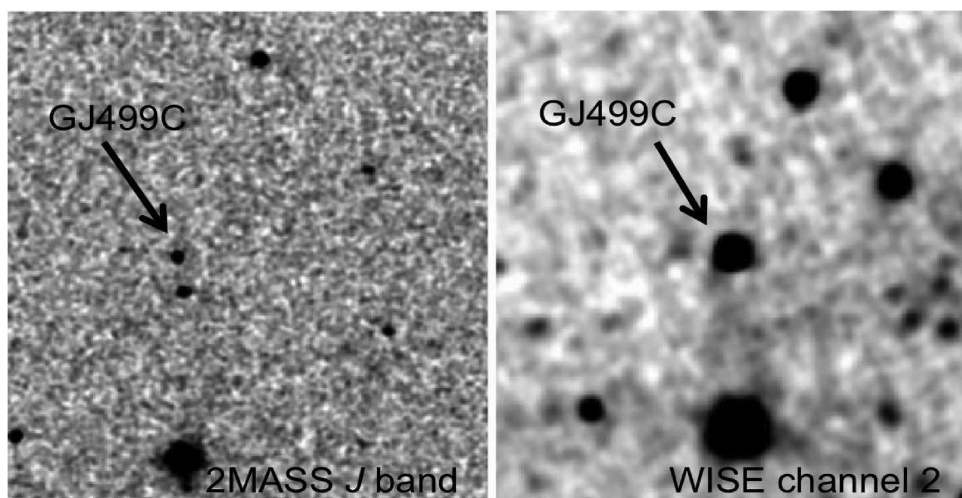


Figure 4. A 5 arcmin \times 5 arcmin finder chart for the GJ499C dwarf. On the left-hand panel is the *J*-band image and on the right-hand panel is the *W2* band. North is up and east is left.

show that the primary is at a distance of 18.80 ± 0.61 pc, and is in agreement with the photometric distance derived for the UCD companion. GJ499C has a on-sky separation of 8.6 arcmin from the primary, or 9708 au. Proper motion measurements come from the van Leeuwen (2007) catalogue and are in agreement with other values published such as Zacharias et al. (2012), Kharchenko & Roeser (2009) and Röser et al. (2008). In order to estimate the physical properties of this system, we follow the same approach as for G255-34AB.

According to the method described in Schlafman & Laughlin (2010), we can use the V and K_s magnitudes of 9.439 and 6.041, respectively (taken from the Hipparcos and 2MASS catalogues) for the K5 dwarf to estimate an $[\text{Fe}/\text{H}] = -0.20 \pm 0.2$, suggestive of a slightly metal poor system. If we do the same calculations for the M4 companion, with $V = 14.90$ and $K_s = 9.55$, the result is $[\text{Fe}/\text{H}] = -0.17 \pm 0.2$. Both results are consistent with a metal poor system.

The velocity components published in Bobylev, Goncharov & Bajkova (2006) place the pair on the edge of the Eggen box, therefore suggesting youth. However, kinematics offers a poor tool to place constraints on ages. West et al. (2008) used the activity lifetimes of M dwarfs to calculate ages, suggesting an age of $4.5_{-1.0}^{+0.5}$ Gyr for M4 dwarfs. We thus consider this as a lower limit to the age of the system.

3.3 Possible contamination

We performed a statistical analysis with the purpose of estimating the probability that these two systems are, in fact, gravitationally bound and are not merely randomly aligned.

First, we estimated the absolute magnitude in the J band for each UCD ± 1 spectral type. We did this using two different methods, first the mean 2MASS M_J as function of spectral type from the Dupuy & Liu (2012) and also from the Marocco et al. (2010) relations between M_J and spectral type. Marocco et al. (2010) uses the MKO photometric system, which we converted to the 2MASS photometry using the Stephens & Leggett (2004) relations. With M_J we estimate a minimum and maximum distance for each L dwarf. We then calculate a conical volume in the sky, with a radius that is defined by the separation between the UCD and its primary companion. For G255-34B, the distances 24.5 and 45.8 pc define a volume of 2.95×10^{-3} pc³, whereas for the GJ499C, 12.6 and 27.0 pc define a volume of 0.116 pc³.

Secondly, we consider the number of stars within these volumes. The luminosity function (Reid, Cruz & Allen 2007) derived from the 8 and 20 pc samples gives us a lower and upper limit for the density of stars in the sky (0.062–0.076 stars pc⁻³). Multiplying this number by the volumes around G255-34B, we expect to find between 1.830×10^{-4} and 2.242×10^{-4} MS stars that could appear as companions to the secondaries. For GJ499C, we would expect between 7.185×10^{-3} and 8.807×10^{-3} stars.

Another important aspect to consider is that, even though stars could lie within the volume around the L dwarfs, only a small fraction could have common proper motion. We therefore analyse the probability of finding Hipparcos and Gliese stars that, by random chance, may have the same motion across the sky as our L dwarfs. In order to do so, we used the initial sample of MS stars with a maximum distance of 50 pc and considered first the ones lying inside a spherical volume with 45° radius. Such a large volume assures that we have enough stars in our sample to estimate the fraction of those that could appear as common proper motion to our secondaries. We have carefully excluded from this region a circular

area where the common proper motion primary companion lies, to avoid counting it as one of the randomly aligned stars. Next, we selected only stars that could masquerade as common proper motion companions to the L dwarfs up to a 2σ detection, which was used in our initial classification as a common proper motion candidate, i.e. within ± 120 mas yr⁻¹ of the value of the secondary (valid for the two L dwarfs).

Finally, taking into account the fraction of stars with similar proper motions as the secondary, and the sky density, we find that for the G255-34B dwarf, an average of 6.40×10^{-6} MS stars could masquerade as a companion to the UCD by random chance, whereas for the GJ499C this value is of 1.36×10^{-4} MS stars. This statistical analysis allows us to say then, with a high degree of confidence, that both systems are genuine associations and not chance alignments to a high degree of significance.

4 DISCUSSION

4.1 Binary fraction

We have gathered information about all of the L dwarfs that are in binary or multiple systems, from the current literature, finding 59 L dwarfs that form part of binary or multiple systems. Of these, 35 are in a system where the primary is another UCD. Two have white dwarfs as primaries and the remaining 22 have an MS star primary. For the purposes of this paper, we only present the latter 22, with information about these systems shown in Table 6. The distance has been estimated using parallax measurements where available or, otherwise, from photometric data.

Considering the two new systems presented here, the sample has now 24 binaries, with six triples and two quadruples. This gives a fraction of 1:4 triple to binary systems and 1:12 quadruples to binary systems. These values differ from the ones presented in Faherty et al. (2010). However, in the latter case the authors considered a wide UCD companion sample containing all UCD binary systems, and not only the ones with L dwarfs as secondaries.

Our initial sample of L dwarf candidates from 2MASS was completed up to a magnitude of 16 in the J band. This is quite similar to the completeness limit of the Point Source catalogue of 2MASS. According to Skrutskie et al. (2006), 2MASS is virtually complete (~ 99 per cent of the sky) to the 10σ sensitivity limit for sources at or fainter than $J = 15.8$. Our sample is thus complete to this limit, and we see that all known L dwarfs with $J < 16$ have turned up in our initial search. Using the relationship between absolute and apparent magnitude (Knapp et al. 2004, Liu et al. 2006 and Marocco et al. 2010), for an L9 dwarf, we estimate that our sample is complete up to a distance of 19 pc (for an L0 this limit would be 94 pc). However, this completeness is only valid for the sky regions surveyed, since we have excluded reddened areas and avoided the Galactic plane.

In order to estimate the number of L dwarfs expected in the full sky, we took a spherical region of space with a radius of 19 pc, and multiplied it by the Cruz et al. (2007) space density estimate L dwarfs ($3.8 \pm 0.6 \times 10^{-3}$ pc⁻³). We estimate that $\sim 109 \pm 17$ L dwarfs should lie within the region studied.

Based on Table 6, we find that six L dwarfs are part of binary systems in which the primary is an MS star, including the GJ 499ABC system presented here. Therefore, we find that the binary fraction for L dwarfs that have MS companions is ~ 6 per cent. Considering now all the Hipparcos and Gliese stars, we find that 1787 were within our area and out to 19 pc. The binary fraction of stars with L dwarfs as wide companions is thus 0.33 per cent. The systems

Table 6. Known binary systems containing one L dwarf secondary.

Name	SpType (Primary)	SpType (Secondary)	Distance (pc) (Primary)	sep (arcsec)	Projected sep (au)	Age (Gyr)	Ref
HD 89744A	F8	L0	39.43 ± 0.48	63	2480	2.1–7.2	4,13,25,32,33
G239-25A	M3	L0	10.73 ± 0.15	2.80	30	–	4,17,25
NLTT2274A	M4	L0	35.00 ± 2.00	23.0	483	4.5–10.0	23
AB PicA	K1	L1	46.06 ± 1.46	5.5	253	0.02–13.8	4,8,25,26,31
HD 16270A	K3.5	L1	21.27 ± 0.43	11.9	254	–	4,7,25
G124-62A	dM4.5	L1+L1	27.48 ± 2.70	44	1452	–	15,16,25
GQ LupA	K7	L1.5	140.00 ± 50.00	0.7	98	3.0	20,23
G73-26A	M2	L2	35.00 ± 3.00	73.0	1898	3–4	23
G196-3A	M3	L2	14.90 ± 2.70	16	243	0.025	11,12,36
GJ618.1A	K7	L2.5	33.42 ± 3.00	35	1170	–	4,13
G62-33A	K0	L3	30.96 ± 0.82	66	2043	4.4	23,26
G200-28A	G5	L4	45.66 ± 1.29	570	2600	4.2–9.0	23,26,27
HD 49197A	F5	L4	44.90 ± 1.21	0.95	44	0.5–4.7	4,9,26,27,28
GJ564A	F9	L4+L4	18.17 ± 0.11	2.64	48	0.05–12.4	4,18,29,30
HD 2057A	F8	L4+L4	43.82 ± 1.69	218	9465	1.6–5.3	4,5,6,23,26,34,37
G1417A	G0+G0	L4.5+L4.5	21.93 ± 0.21	90	1953	0.08–3.2	14,15,27,29
GJ1001A	M3.5	L4.5+L4.5	13.01 ± 0.67	18.6	180	–	1,2,3,25
G203-50A	M4.5	L5	22.40 ± 1.90	6.4	135	–	21
LP 261-75A	M4.5	L6	62.15 ± 28.58	13	450	0.04	10,12,25
HD 203030A	G8	L7.5	40.88 ± 1.24	11.9	487	0.25–1.4	4,22,25,26,28
G1584A	G0+G3	L8	17.86 ± 0.25	194	3465	3.3–4.8	19,26,34
G1337A	G8+K1	L8+T0	20.36 ± 0.22	43	875	13.8	13,24,26
G255-34A	K8	L2	35.87 ± 149	38.0	1364	–	38
GJ499AB	K7+M4	L5	18.80 ± 0.61	516	9708	–	38

References: (1) Golimowski et al. (2004); (2) Martin, Brandner & Basri (1999); (3) Henry et al. (2006); (4) Anderson & Francis (2011); (5) Liu, Dupuy & Leggett (2010); (6) Cruz et al. (2007); (7) Gizis et al. (2001); (8) Chauvin et al. (2005); (9) Metchev & Hillenbrand (2004); (10) Reid & Walkowicz (2006); (11) Rebolo et al. (1998); (12) Shkolnik, Liu & Reid (2009); (13) Wilson et al. (2001); (14) Kirkpatrick et al. (2001); (15) Bouy et al. (2003); (16) Seifahrt, Guenther & Neuhäuser (2005); (17) Forveille et al. (2004); (18) Potter et al. (2002); (19) Mugrauer, Seifahrt & Neuhäuser (2007); (20) Neuhäuser et al. (2005); (21) Radigan et al. (2008); (22) Metchev & Hillenbrand (2006); (23) Faherty et al. (2010); (24) Burgasser, Kirkpatrick & Lowrance (2005); (25) Dupuy & Liu (2012); (26) Casagrande et al. (2011); (27) Holmberg, Nordström & Andersen (2009); (28) Wright et al. (2004); (29) Lafrenière et al. (2007); (30) Lambert & Reddy (2004); (31) Tetzlaff, Neuhäuser & Hohle (2011) (32) Edvardsson et al. (1993); (33) Bryden et al. (2009); (34) Marsakov & Shevelev (1995); (35) Reid et al. (2003); (36) Zapatero Osorio et al. (2010); (37) Reid et al. (2006); (38) this paper.

considered for this analysis have separations between 30 and 10 000 au. It is worth noting that the two systems with smaller on-sky and physical separations, G 239-25AB and GJ 564AB (with separations of 30 and 48 au, respectively), have been discovered with adaptive optics, since finding such faint objects so close to bright stars is rather difficult.

If we now analyse the sample of known L dwarfs (based on Dwarf Archives), and do not take into account any distance constraints, we see that the binary fraction of L dwarfs in any kind of system goes up to ~ 10 per cent. However, only 4 per cent of L dwarfs have MS stars as companions. We have not considered any possible unresolved binaries, and hence the values presented are just a lower estimate. The binary fractions here derived are not affected by the Malmquist bias, since both the number of single L dwarfs and the number of those found to be in multiple systems are affected in the same way.

4.2 Unresolved binaries

In order to identify any possible unresolved binaries in the sample presented in Table 6, we take advantage of the associated high-quality parallax measurements that can be inferred for the companion L dwarfs in known multiple systems. We plotted the spectral type of the L dwarf components versus their M_J (Fig. 5). To estimate the absolute magnitude, we used the primaries dis-

tances. We excluded from this analysis two objects, GQ LupB (J15491209–3539039) and HD 203030B (J21185897+2613461) since they do not have 2MASS J -band measurements. Also, we have plotted the G124-62BC components as an unresolved binary, since there are no individual photometric measurements of the two L1 components. The other five systems in which an MS star has two UCDS as secondaries are all resolved, and in Fig. 5 we plot the two components with different symbols, open circle and open triangle and numbered. The two new benchmark systems presented here are shown as filled circles. The filled squares are L dwarf companions that have not previously been considered as possible unresolved multiples.

One interesting case is G196-3B. The distance to this L2 dwarf has been estimated by many different authors. Shkolnik et al. (2009) uses the companion, an M3 dwarf, to infer a photometric distance of 14.9 ± 2.7 pc to the system (Reid et al. 2002, 2007). Faherty et al. (2009), on the other hand, uses 2MASS M_J versus spectral type relationships from Cruz et al. (2003) to derive a different distance for this L2 dwarf, 32.0 ± 2.0 pc. More recently, Zapatero Osorio et al. (2010) discuss the system in detail giving minimum and maximum values for its distance of 15 and 51 pc, respectively. These two limits are given for two different scenarios, first if we consider the primary to be a single object and a field star, and secondly if we consider the secondary to actually be a double object with ages of 3 Myr. Adopting a probable distance range of 15–30 pc [as Zapatero

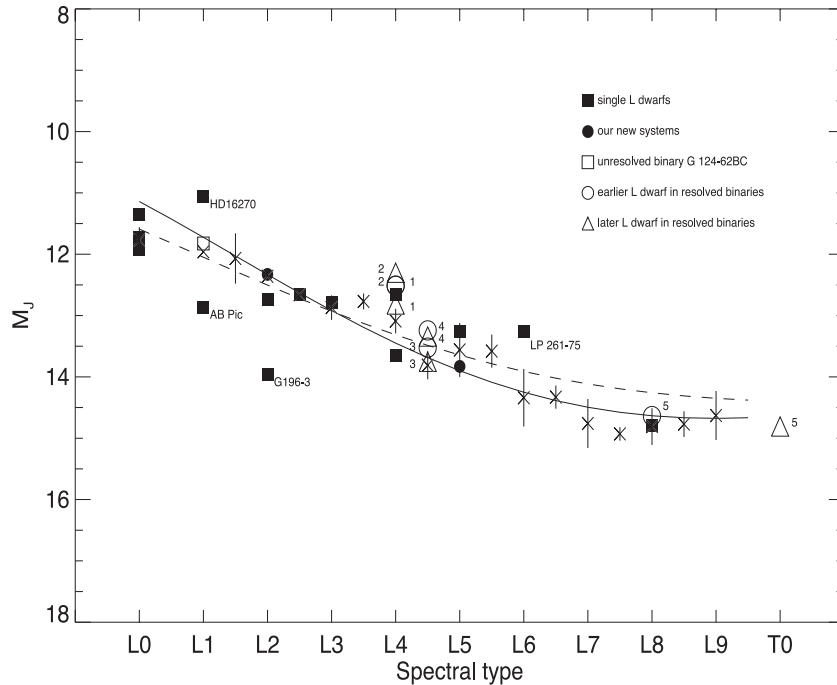


Figure 5. Spectral type versus M_J for the L dwarf+MS star systems in Table 6. The filled squares indicate those systems with only one L dwarf, the filled circles the two new systems presented in this paper. The systems in which there are two unresolved L dwarfs and an MS star are represented by two symbols, an open circle showing the earlier of the two UCDs and an open triangle showing the later type UCD. The dashed line shows the polynomial fit from Faherty et al. (2012) and the solid one the fit from Marocco et al. (2010). The crosses represent the mean 2MASS M_J for each spectral type (Dupuy & Liu 2012). The numbers represent the following systems: (1) GJ564ABC; (2) HD 2057ABC; (3) G1417ABCD; (4) GJ1001ABC; (5) G1337ABCD.

Osorio et al. (2010) conclude and in accordance with the Faherty et al. (2009) and Shkolnik et al. (2009), values], we estimate an M_J between 12.4 and 13.9. In Fig. 5, we have plotted the latter value, since this places the L2 dwarf further away from the polynomial fits. It can be seen that this particular dwarf shows redder colours than expected for its spectral type, as noted in Zapatero Osorio et al. (2010) (this is true even if we consider the dwarf to be an L3, as Zapatero Osorio et al. 2010). The reason for this is still to be fully explained, although Zapatero Osorio et al. (2010) suggest that the object might have a low-gravity atmosphere with upper atmospheric layers or a warm dusty envelope.

The L dwarf companion to AB PicA has been previously reported as underluminous (Faherty et al. 2009). This is a young system, with ages smaller than 1 Gyr, and a low-gravity dwarf. We note though that the unresolved binary G124-62BC, open square in Fig. 5, does not sit above the expected position in the spectral type versus M_J plot. This could perhaps suggest that the actual single object sequence is slightly below the best-fitting sequences plotted, in which case AB PicB would not be underluminous, but making the position of HD 16270B stand out even more as an overluminous object. Just like HD 16270B, LP 261-75B appears to be slightly overluminous for its spectral type. However, if we take into account uncertainties in the spectral type of ± 1 , we see that they both fit the sequence.

Another interesting object is the system with HD 2057A as primary, and two resolved L4 dwarfs as secondaries (number 2 in Fig. 5). First mentioned in Reid et al. (2006), the two L4 dwarfs are later confirmed as companions to the F8 star in Faherty et al. (2010). As can be seen in the plot, the two symbols sit well above the average M_J for typical L4 dwarfs. In fact, one of the dwarfs has $M_J \sim 1.15$ above the value given by the polynomial fit of Marocco et al. (2010) and 1.01 above the one by Faherty et al. (2012). This

is not reported as a young system (Casagrande et al. 2011), and therefore the overluminosity might be explained by multiplicity. In such case, we could be looking at a quadruple system of L dwarfs. Only with further observations can we expect to truly explain this system. In the same way, the GJ564 system also appears to have one of the two L4 secondaries above the sequence, and again binarity could be the explanation for its position in the plot.

5 CONCLUSIONS

Using the all-sky surveys 2MASS and WISE, we have identified two new systems with an L dwarf and an MS star as the primary components. Such benchmark systems allow us to better understand how the observed properties of UCDs are dependent on their ages and metallicities, and the two new systems presented here will help populate the growing sample of brown dwarfs with well-constrained properties. Spectroscopy of the two primaries will be needed in the future to further estimate their ages and metallicities, thus fully characterizing the systems.

We have also investigated the binary fraction for the specific type of binaries presented here, those in which the L dwarf has an FGK or M star as a wide companion. The number of such systems known to date is, however, small and any conclusions are dependent on the completeness of the sample, in this case, up to distances of 19 pc. The use of deeper surveys such as UKIDSS and Visible and Infrared Survey Telescope for Astronomy (VISTA, Irwin et al. 2004) will allow us to probe further distances and expand the number of such systems. Considering that 2MASS is complete up to a $J = 16$, and taking into account the number of L dwarfs found, one can expect that by going three orders of magnitude fainter in the

mentioned surveys we can expect to increase the volume of sky sampled by up to 30 times. This means that we can expect to find around 500 times more L dwarfs having an MS star as a companion in an all sky sample. Ultimately, it is by studying a large sample of UCDS with abundances and age constraints from their companions that we can further understand and improve current atmospheric models of these objects.

Finally, we show that some of the L dwarfs present in systems with an MS star could be unresolved binaries, due to their relative overluminosity for their spectral type. One interesting case is the HD 2057 system, in which two resolved L4 dwarfs might actually be unresolved binaries themselves, thus making this a possible quadruple L dwarf system with an F8 star as the primary.

ACKNOWLEDGEMENTS

JG and ACD-J are supported by RoPACS, a Marie Curie Initial Training Network funded by the European Commission's Seventh Framework Programme. ACD-J is also supported by a FONDECYT postdoctorado fellowship under project no. 3100098. DP, ZZ and HJ have received support from RoPACS during this research. This research has benefited from the M, L, and T dwarf compendium housed at DwarfArchives.org and maintained by Chris Gelino, Davy Kirkpatrick and Adam Burgasser. This publication makes use of data products from the 2MASS, which is a joint project of the University of Massachusetts and the IPAC/Caltech, funded by NASA and the National Science Foundation. We have also made use of data products from *WISE*, which is a joint project of the University of California, Los Angeles, and the Jet Propulsion Laboratory/California Institute of Technology, funded by the National Aeronautics and Space Administration. This research has made use of the SIMBAD data base, operated at CDS, Strasbourg, France. This research has made use of data obtained from the SuperCOSMOS Science Archive, prepared and hosted by the Wide Field Astronomy Unit, Institute for Astronomy, University of Edinburgh, which is funded by the UK Science and Technology Facilities Council. We thank Tom Marsh for the use of PAMELA and MOLLY. Based on observations made with the Italian Telescopio Nazionale Galileo (TNG) operated on the island of La Palma by the Fundacin Galileo Galilei of the INAF (Istituto Nazionale di Astrofisica) at the Spanish Observatorio del Roque de los Muchachos of the Instituto de Astrofisica de Canarias.

REFERENCES

Anderson E., Francis C., 2011, *VizieR Online Data Catalog*, 5137, 0
 Baraffe I., Chabrier G., Allard F., Hauschildt P. H., 1998, *A&A*, 337, 403
 Bobilev V. V., Goncharov G. A., Bajkova A. T., 2006, *Astron. Rep.*, 50, 733
 Bouy H., Brandner W., Martín E. L., Delfosse X., Allard F., Basri G., 2003, *AJ*, 126, 1526
 Bryden G. et al., 2009, *ApJ*, 705, 1226
 Burgasser A. J., Kirkpatrick J. D., Lowrance P. J., 2005, *AJ*, 129, 2849
 Burningham B. et al., 2009, *MNRAS*, 395, 1237
 Casagrande L., Schoenrich R., Asplund M., Cassisi S., Ramirez I., Melendez J., Bensby T., Feltzing S., 2011, *VizieR Online Data Catalog*, 353, 9138
 Casewell S. L., Jameson R. F., Burleigh M. R., 2008, *MNRAS*, 390, 1517
 Chauvin G. et al., 2005, *A&A*, 438, L29
 Cruz K. L., Reid I. N., Liebert J., Kirkpatrick J. D., Lowrance P. J., 2003, *AJ*, 126, 2421
 Cruz K. L. et al., 2007, *AJ*, 133, 439
 Cushing M. C. et al., 2008, *ApJ*, 678, 1372
 Cushing M. C. et al., 2011, *ApJ*, 743, 50
 Day-Jones A. C. et al., 2011, *MNRAS*, 410, 705

Delfosse X. et al., 1997, *A&A*, 327, L25
 Dupuy T. J., Liu M. C., 2012, *ApJS*, 201, 19
 Edvardsson B., Andersen J., Gustafsson B., Lambert D. L., Nissen P. E., Tomkin J., 1993, *A&A*, 275, 101
 Eggen O. J., Iben I. Jr, 1989, *AJ*, 97, 431
 Epchtein N. et al., 1997, *The Messenger*, 87, 27
 Faherty J. K., Burgasser A. J., Cruz K. L., Shara M. M., Walter F. M., Gelino C. R., 2009, *AJ*, 137, 1
 Faherty J. K., Burgasser A. J., West A. A., Bochanski J. J., Cruz K. L., Shara M. M., Walter F. M., 2010, *AJ*, 139, 176
 Faherty J. K. et al., 2012, *ApJ*, 752, 56
 Forveille T. et al., 2004, *A&A*, 427, L1
 Giclas H. L., Burnham R., Thomas N. G., 1971, Lowell proper motion survey Northern Hemisphere. The G numbered stars. 8991 stars fainter than magnitude 8 with motions $> 0''.26/\text{year}$. Lowell Observatory, Flagstaff
 Gizis J. E., Kirkpatrick J. D., Wilson J. C., 2001, *AJ*, 121, 2185
 Gliese W., Jahreiss H., 1991, NASA STI/Recon Technical Report A, 92, 33932
 Golimowski D. A. et al., 2004, *AJ*, 128, 1733
 Henry T. J., Jao W.-C., Subasavage J. P., Beaulieu T. D., Ianna P. A., Costa E., Méndez R. A., 2006, *AJ*, 132, 2360
 Holmberg J., Nordström B., Andersen J., 2009, *A&A*, 501, 941
 Hubeny I., Burrows A., 2007, *ApJ*, 669, 1248
 Irwin M. J. et al., 2004, *SPIE*, 5493, 411
 Jameson R. F., Casewell S. L., Bannister N. P., Lodieu N., Keresztes K., Dobbie P. D., Hodgkin S. T., 2008, *MNRAS*, 384, 1399
 Jones H. R. A., Steele I. A., 2001, *Ultracool Dwarfs - New Spectral Types L and T*. Springer, Heidelberg
 Kharchenko N. V., Roeser S., 2009, *VizieR Online Data Catalog*, 1280, 0
 Kirkpatrick J. D., 2005, *ARA&A*, 43, 195
 Kirkpatrick J. D. et al., 1999, *ApJ*, 519, 802
 Kirkpatrick J. D., Dahn C. C., Monet D. G., Reid I. N., Gizis J. E., Liebert J., Burgasser A. J., 2001, *AJ*, 121, 3235
 Kirkpatrick J. D. et al., 2011, *ApJS*, 197, 19
 Kirkpatrick J. D. et al., 2012, *ApJ*, 753, 156
 Knapp G. R. et al., 2004, *AJ*, 127, 3553
 Lafrenière D. et al., 2007, *ApJ*, 670, 1367
 Lambert D. L., Reddy B. E., 2004, *MNRAS*, 349, 757
 Lawrence A. et al., 2007, *MNRAS*, 379, 1599
 Leggett S. K., 1992, *ApJS*, 82, 351
 Liu M. C., Leggett S. K., Golimowski D. A., Chiu K., Fan X., Geballe T. R., Schneider D. P., Brinkmann J., 2006, *ApJ*, 647, 1393
 Liu M. C., Dupuy T. J., Leggett S. K., 2010, *ApJ*, 722, 311
 Lucas P. W. et al., 2010, *MNRAS*, 408, L56
 Luyten W. J., 1979, *A Catalogue of Stars with Proper Motion $> 0''.5$ Annually (LHS)*. Univ. Minnesota, Minneapolis
 Marocco F. et al., 2010, *A&A*, 524, A38
 Marsakov V. A., Shevelev Y. G., 1995, *VizieR Online Data Catalog*, 5089, 0
 Martin E. L., Brandner W., Basri G., 1999, *Sci*, 283, 1718
 Metchev S. A., Hillenbrand L. A., 2004, *ApJ*, 617, 1330
 Metchev S. A., Hillenbrand L. A., 2006, *ApJ*, 651, 1166
 Mugrauer M., Seifahrt A., Neuhäuser R., 2007, *MNRAS*, 378, 1328
 Neuhäuser R., Guenther E. W., Wuchterl G., Mugrauer M., Bedalov A., Hauschildt P. H., 2005, *A&A*, 435, L13
 Pinfield D. J., Jones H. R. A., Lucas P. W., Kendall T. R., Folkes S. L., Day-Jones A. C., Chappelle R. J., Steele I. A., 2006, *MNRAS*, 368, 1281
 Pinfield D. J. et al., 2012, *MNRAS*, 422, 1922
 Potter D., Martín E. L., Cushing M. C., Baudoz P., Brandner W., Guyon O., Neuhäuser R., 2002, *ApJ*, 567, L133
 Radigan J., Lafrenière D., Jayawardhana R., Doyon R., 2008, *ApJ*, 689, 471
 Rebolo R., Zapatero Osorio M. R., Madrugá S., Bejar V. J. S., Arribas S., Licandro J., 1998, *Sci*, 282, 1309
 Reid I. N., Walkowicz L. M., 2006, *PASP*, 118, 671
 Reid I. N., Kirkpatrick J. D., Liebert J., Gizis J. E., Dahn C. C., Monet D. G., 2002, *AJ*, 124, 519

- Reid I. N. et al., 2003, *AJ*, 126, 3007
Reid I. N. et al., 2004, *AJ*, 128, 463
Reid I. N., Lewitus E., Allen P. R., Cruz K. L., Burgasser A. J., 2006, *AJ*, 132, 891
Reid I. N., Cruz K. L., Allen P. R., 2007, *AJ*, 133, 2825
Roeser S., Demleitner M., Schilbach E., 2010, *AJ*, 139, 2440
Röser S., Schilbach E., Schwan H., Kharchenko N. V., Piskunov A. E., Scholz R.-D., 2008, *A&A*, 488, 401
Salim S., Gould A., 2003, *ApJ*, 582, 1011
Schlaufman K. C., Laughlin G., 2010, *A&A*, 519, A105
Schmidt S. J., West A. A., Hawley S. L., Pineda J. S., 2010, *AJ*, 139, 1808
Seifahrt A., Guenther E., Neuhäuser R., 2005, *A&A*, 440, 967
Shkolnik E., Liu M. C., Reid I. N., 2009, *ApJ*, 699, 649
Skrutskie M. F. et al., 2006, *AJ*, 131, 1163
Stephens D. C., Leggett S. K., 2004, *PASP*, 116, 9
Tetzlaff N., Neuhäuser R., Hohle M. M., 2011, *MNRAS*, 410, 190
van Biesbroeck G., 1961, *AJ*, 66, 528
van Leeuwen F., 2007, *A&A*, 474, 653
Vyssotsky A. N., 1956, *AJ*, 61, 201
Weis E. W., 1991, *AJ*, 101, 1882
West A. A., Hawley S. L., Bochanski J. J., Covey K. R., Reid I. N., Dhital S., Hilton E. J., Masuda M., 2008, *AJ*, 135, 785
Wilson J. C., Kirkpatrick J. D., Gizis J. E., Skrutskie M. F., Monet D. G., Houck J. R., 2001, *AJ*, 122, 1989
Wright J. T., Marcy G. W., Butler R. P., Vogt S. S., 2004, *ApJS*, 152, 261
Wright E. L. et al., 2010, *AJ*, 140, 1868
York D. G. et al., 2000, *AJ*, 120, 1579
Zacharias N., Monet D. G., Levine S. E., Urban S. E., Gaume R., Wycoff G. L., 2005, *VizieR Online Data Catalog*, 1297, 0
Zacharias N., Finch C. T., Girard T. M., Henden A., Bartlett J. L., Monet D. G., Zacharias M. I., 2012, *VizieR Online Data Catalog*, 1322, 0
Zapatero Osorio M. R., Rebolo R., Bihain G., Béjar V. J. S., Caballero J. A., Álvarez C., 2010, *ApJ*, 715, 1408

This paper has been typeset from a $\text{\TeX}/\text{\LaTeX}$ file prepared by the author.